



# COMPARISON AMONG EQUIVALENT STRESS PREDICTIONS BASED ON SPHERICAL, ELLIPSOIDAL AND PRISMATIC HULLS<sup>1</sup>

Marco Antonio Meggiolaro<sup>2</sup>  
 Jaime Tupiassú Pinho de Castro<sup>2</sup>

## Abstract

Non-proportional (NP) multiaxial fatigue life predictions require the calculation of equivalent stress ranges associated with the history path. A traditional way to find such ranges is to use spherical, ellipsoidal or prismatic hull methods, which search for enclosures of the entire history path in stress diagrams. In this work, all existing hull methods are presented and compared using results from more than 3,000,000 Monte Carlo simulations of random and especially chosen path topologies in two to five-dimensional stress diagrams. New models are also proposed, based on Deperrois' idea of longest chords. It is found that the proposed models are very similar to the Maximum Prismatic Hull model, but with a much simpler and efficient algorithm to compute equivalent stresses. It is also shown that the Minimum Circumscribed Ellipsoid, Minimum Volume Ellipsoid, and Minimum Ball (MB) methods may result in very poor predictions of the stress amplitudes. The only recommended method based on ellipsoids is the Minimum F-norm Ellipsoid (MFE) which, together with the Maximum Prismatic Hull model and its variations, are very efficient to predict equivalent amplitudes in NP histories. Experimental results for 15 different multiaxial histories are also used to evaluate the discussed methods.

**Keywords:** Multiaxial fatigue; Equivalent stress; Convex hull.

## COMPARAÇÃO ENTRE PREDIÇÕES DE TENSÃO EQUIVALENTE BASEADAS EM ENVOLTÓRIAS ESFÉRICAS, ELIPSOIDAIS E PRISMÁTICAS

### Resumo

Predições de vida à fadiga sob cargas multiaxiais não-proporcionais (NP) requerem o cálculo das amplitudes equivalentes de tensão associadas ao caminho da história. Uma forma de encontrar essas amplitudes consiste de usar métodos baseados em envoltórias esféricas, elípticas ou prismáticas, que procuram por envoltórias que contêm em seu interior toda a história de tensão. Neste trabalho, todos os métodos existentes baseados em envoltórias convexas são apresentados e comparados, usando resultados de mais de 3.000.000 de simulações de Monte Carlo em caminhos aleatórios ou especialmente escolhidos em diagramas de duas a cinco dimensões. Novos modelos são propostos, baseados na idéia de Deperrois das cordas mais longas. Conclui-se que os métodos propostos são muito similares ao método da Máxima Envoltória Prismática, mas com um algoritmo muito mais simples e eficiente para computar tensões equivalentes. Mostra-se também que os métodos da Mínima Envoltória Elipsoidal, Elipsóide de Mínimo Volume, e Mínima Esfera podem resultar em predições ruins das amplitudes de tensão. O único método recomendado baseado em elipsóides é o Elipsóide de Mínima Norma-F que, junto com o modelo da Máxima Envoltória Prismática e suas variações, são muito eficientes para prever amplitudes equivalentes em histórias NP. Resultados experimentais para 15 histórias multiaxiais diferentes são usados para avaliar os métodos apresentados.

**Palavras-chave:** Fadiga multiaxial; Tensão equivalente; Envoltória convexa.

<sup>1</sup> Technical contribution to 66<sup>th</sup> ABM Annual Congress, July, 18<sup>th</sup> to 22<sup>th</sup>, 2011, São Paulo, SP, Brazil.

<sup>2</sup> Engenheiro Mecânico, Ph.D., Professor Dept. Eng. Mecânica, PUC-Rio.

## 1 INTRODUCTION

Long-life multiaxial fatigue damage models are based on stress ranges such as the octahedral shear stress range  $\Delta\tau_{Mises}$ , the shear range  $\Delta\tau(\theta)$  projected onto a candidate plane with direction  $\theta$ , or the maximum shear range  $\Delta\tau_{max}$ . It is not difficult to define these ranges for constant amplitude loadings, where only two stress states need to be considered, one associated with the peak and the other with the valley.<sup>(1-3)</sup>

However, for multiaxial variable amplitude (VA) loadings, in special when the history is non-proportional (NP), it is not clear how these ranges should be defined and identified. The loading path, represented e.g. in a Mises diagram, could have a generic curved shape spanning infinitely many stress states, without a clear peak or valley. The following sections deal with how to quantify the stress ranges used by the various multiaxial damage models, associated with variable amplitude (VA) non-proportional (NP) histories that are periodic in time.

Consider that the periodic history is formed by repeatedly following a given loading path domain  $D$ , where  $D$  contains all points from the stress variations along one period of the history. For Case A cracks (Figure 1), after projecting  $D$  onto a candidate plane perpendicular to the specimen surface (i.e. with  $\phi = 90^\circ$  from Figure 1), the maximum shear stress variation  $\Delta\tau_{max}$  is basically the difference between the maximum and minimum values along  $D$  of the shear stress  $\tau_A$  that acts parallel both to the surface and to the critical plane. The approach is similar for strain-based methods.

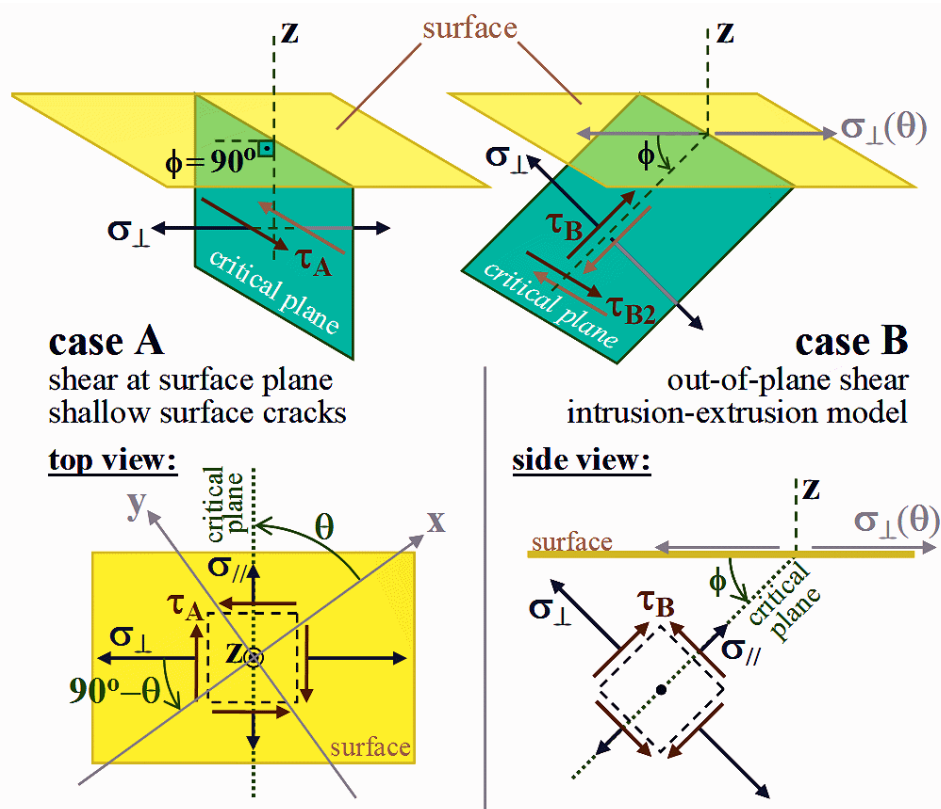
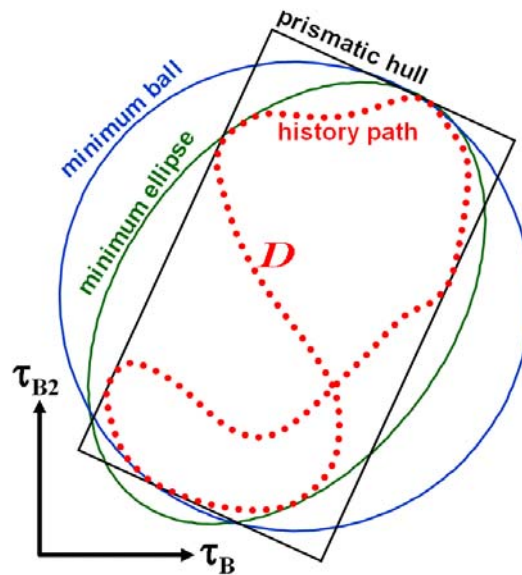


Figure 1: Case A and Case B cracks.

But, for Case B cracks (Figure 1), the effective  $\Delta\tau_{max}$  is not easy to define, since a generic NP loading path  $D$  results in NP variations of both shear stresses  $\tau_B$  and  $\tau_{B2}$  that act parallel to the critical plane. Both  $\tau_B$  and  $\tau_{B2}$  influence the growth of Case B shear cracks along the critical plane, therefore  $\tau_{B2}$  should not be neglected. To calcu-

late the maximum strain range  $\Delta\tau_{max}$  at the critical plane considering  $\tau_{B2}$ , it is necessary to draw the path  $D$  of the stress history along a  $\tau_B \times \tau_{B2}$  diagram, as shown in Figure 2.



**Figure 2:** Stress history path  $D$  in the  $\tau_B \times \tau_{B2}$  diagram, enclosed in convex hulls based on circles (balls), ellipses and rectangular prisms.

For a complex-shaped history such as the one shown in the figure, it is not easy to decide how to obtain the effective  $\Delta\tau_{max}$ . The so-called convex hull methods [4-8] try to find circles, ellipses or rectangles that contain the entire path (in the 2D case). In a nutshell, in the 2D case, the Minimum Ball (MB) method<sup>(4)</sup> searches for the circle with minimum radius that contains  $D$ , the minimum ellipse methods<sup>(5-7)</sup> search for an ellipse with semi-axes  $a$  and  $b$  that contains  $D$  with minimum area  $\pi \cdot a \cdot b$  or minimum norm  $(a^2 + b^2)^{1/2}$ ; and the maximum prismatic hull methods<sup>(6,8)</sup> search among the smallest rectangles that contain  $D$  the one with maximum area or maximum diagonal (it's a max-min search problem). The value of  $\Delta\tau_{max}$  in Figure 2 would either be assumed as the value of the circle diameter, or twice the ellipse norm, or the rectangle diagonal.

The convex hull methods can also be applied to traction-torsion histories, if a  $\sigma_x \times \tau_{xy}\sqrt{3}$  diagram is considered. The effective range in this case is the Mises stress range  $\Delta\sigma_{Mises}$ , defined in the next section.

Such convex hull methods can be extended to histories involving more than two stress components. E.g., if the history path is plotted in a 3D diagram representing 3 stress components, the convex hull methods will search for spheres, ellipsoids or rectangular prisms. For higher dimension diagrams, the search is for hyperspheres, hyperellipsoids, and rectangular hyperprisms. However, this practice can lead to significant errors, since each convex hull will reflect an effective range calculated on different planes at different points in time. The recommended approach for general 6D histories involving all stress components is then to project them onto Case A and Case B candidate planes, resulting in each case in searches for effective ranges in 2D diagrams  $\sigma \times \tau\sqrt{3}$  or  $\tau_B \times \tau_{B2}$ .

The convex hull methods are described in detail in the following sections. Their framework is based on deviatoric stress diagrams and Mises stress parameters, which are discussed next.

## 2 MISES STRESS PARAMETERS

The methods to obtain effective (or equivalent) stress ranges usually make use of stress parameters based on the Mises yield function. For linear elastic histories, both Mises effective stress  $\sigma_{Mises}$  and Mises (or octahedral) shear stress  $\tau_{Mises}$  can be used as auxiliary parameters, where

$$\sigma_{Mises} = \frac{3}{\sqrt{2}} \tau_{Mises} = \frac{1}{\sqrt{2}} \sqrt{(\sigma_x - \sigma_y)^2 + (\sigma_y - \sigma_z)^2 + (\sigma_x - \sigma_z)^2 + 6(\tau_{xy}^2 + \tau_{yz}^2 + \tau_{xz}^2)} \quad (1)$$

Since the Mises stress  $\sigma_{Mises}$  (as well as the octahedral shear stress  $\tau_{Mises}$ ) equation is always positive, a Mises stress range  $\Delta\sigma_{Mises}$  (also known as relative Mises stress  $\sigma_{RMises}$ ) should be used to correctly evaluate the variation of  $\sigma_{Mises}$  due to a change  $(\Delta\sigma_x, \Delta\sigma_y, \Delta\sigma_z, \Delta\tau_{xy}, \Delta\tau_{xz}, \Delta\tau_{yz})$  in the stress components along some loading path  $\Delta$ :

$$\Delta\sigma_{Mises} = \sigma_{RMises} = \frac{\sqrt{(\Delta\sigma_x - \Delta\sigma_y)^2 + (\Delta\sigma_x - \Delta\sigma_z)^2 + (\Delta\sigma_y - \Delta\sigma_z)^2 + 6(\Delta\tau_{xy}^2 + \Delta\tau_{xz}^2 + \Delta\tau_{yz}^2)}}{\sqrt{2}} \quad (2)$$

Note that the Mises stress range correlates with the octahedral shear range parameter  $\Delta\tau_{Mises}$  through  $\Delta\sigma_{Mises} = \Delta\tau_{Mises} \cdot 3/\sqrt{2}$ .

Note that the octahedral shear range  $\Delta\tau_{Mises}$  is measured on the octahedral planes, it is not equal to twice the shear amplitude  $\tau_a$  acting on the considered plane. But this shear amplitude could be easily obtained by

$$\tau_a = \frac{\sqrt{6}}{4} \Delta\tau_{Mises} = \frac{\sqrt{3}}{6} \Delta\sigma_{Mises} \quad (3)$$

## 3 REDUCED ORDER STRESS SPACES

When dealing with incremental plasticity, it is convenient to represent the stresses in a 9-dimensional (9D) space. In particular, when representing the deviatoric stress tensor in 9D, its norm  $|\bar{S}|$  becomes directly proportional to the Mises stress and octahedral (or Mises) shear stress. But, to find effective ranges in VA-NP histories, it is a good idea to work in a space with reduced dimensions, saving computational effort without modifying the results. The reduction from 9D to 6D deviatoric stresses is simply a matter of eliminating the  $\tau_{yx}$ ,  $\tau_{zx}$  and  $\tau_{zy}$  components from the deviatoric stress tensor, which are redundant because  $\tau_{yx} \equiv \tau_{xy}$ ,  $\tau_{zx} \equiv \tau_{xz}$ , and  $\tau_{zy} \equiv \tau_{yz}$ .

Since the deviatoric stresses  $S_x$ ,  $S_y$  and  $S_z$  are linear-dependent, because  $S_x + S_y + S_z = 0$ , it is possible to further reduce the deviatoric stress dimension from 6D to 5D. There are infinite ways to do this, for example replacing the stresses  $S_x$ ,  $S_y$  and  $S_z$  by new variables  $S_1 \equiv a_{x1} \cdot S_x + a_{y1} \cdot S_y + a_{z1} \cdot S_z$  and  $S_2 \equiv a_{x2} \cdot S_x + a_{y2} \cdot S_y + a_{z2} \cdot S_z$ , where the user-defined coefficients  $a_{x1}$ ,  $a_{y1}$ ,  $a_{z1}$ ,  $a_{x2}$ ,  $a_{y2}$  and  $a_{z2}$  are any values that make the vectors  $[a_{x1} \ a_{y1} \ a_{z1}]^T$ ,  $[a_{x2} \ a_{y2} \ a_{z2}]^T$ , and  $[1 \ 1 \ 1]^T$  become linear independent. A notable example of such transformation is the one with  $[a_{x1} \ a_{y1} \ a_{z1}]^T = [\sqrt{3}/2 \ 0 \ 0]^T$  and  $[a_{x2} \ a_{y2} \ a_{z2}]^T = [0 \ 0.5 \ -0.5]^T$ , resulting in a reduced-order deviatoric stress tensor  $\bar{S}'$  represented in a 5D transformed Euclidean stress-space  $E_{5\sigma}$ , where

$$\begin{cases} \bar{S}' = [S_1 & S_2 & S_3 & S_4 & S_5]^T \\ S_1 = \sigma_x - \frac{\sigma_y}{2} - \frac{\sigma_z}{2} = \frac{3}{2}S_x, & S_2 = \frac{\sigma_y - \sigma_z}{2}\sqrt{3} = \frac{S_y - S_z}{2}\sqrt{3} \\ S_3 = \tau_{xy}\sqrt{3}, & S_4 = \tau_{xz}\sqrt{3}, & S_5 = \tau_{yz}\sqrt{3} \end{cases} \quad (4)$$

The above defined 5D deviatoric stress  $\bar{S}'$  has three very interesting properties:

1) The norm of the 5D vector  $\bar{S}'$  from the  $E_{5\sigma}$  transformed deviatoric stress-space is equal to the Mises equivalent stress  $\sigma_{Mises}$ .

2) The Euclidean distance in the 5D  $E_{5\sigma}$  stress-space between any 2 points  $\bar{S}'_A = [S_{1A} \ S_{2A} \ S_{3A} \ S_{4A} \ S_{5A}]^T$  and  $\bar{S}'_B = [S_{1B} \ S_{2B} \ S_{3B} \ S_{4B} \ S_{5B}]^T$ , respectively associated with the 9D deviatoric stresses  $\bar{S}_A$  and  $\bar{S}_B$ , is equal to the Mises stress range  $\Delta\sigma_{Mises}$  between these stress states.

3) The locus of the points which have the same  $\Delta\sigma_{Mises}$  with respect to a point  $\bar{S}'$  in the  $E_{5\sigma}$  deviatoric stress-space is the surface of a hypersphere with center in  $\bar{S}'$  and radius  $\Delta\sigma_{Mises}$ . This is a simple corollary from the second property.

Note that, for unnotched specimens under histories combining uniaxial tension  $\sigma_x$  and torsion  $\tau_{xy}$ , the 5D deviatoric stress  $\bar{S}'$  can be represented in the classical diagram  $\sigma_x \times \tau_{xy}\sqrt{3}$  using the 2D projection  $[S_1 \ S_3]^T$ , since in this case  $S_1 = \sigma_x$ ,  $S_3 = \tau_{xy}\sqrt{3}$ , and  $S_2 = S_4 = S_5 = 0$ .

After defining all involved stress parameters, the convex hull methods are discussed. These methods are based on convex hulls enclosing the history path in the above defined stress sub-spaces. There are 3 usual types of convex hulls: balls, ellipsoids and rectangular prisms. The Minimum Ball method is presented next.

#### 4 MINIMUM BALL METHOD

Dang Van and Papadoulos<sup>(4)</sup> realized that the search for an effective stress range must take place on the deviatoric stress space. For periodic elastic histories, the mesoscopic stresses and strains in the critically oriented grain should stabilize by the process of elastic shakedown, generating a local residual stress  $[\sigma_{ij}]_{res}$  at such critical grain. Dang Van assumed that the subsequent mesoscopic ( $\mu$ ) stress history at such grain, after the stabilization, is related to the macroscopic ( $M$ ) history through

$$[\sigma_{ij}(t)]_{\mu} = [\sigma_{ij}(t)]_M + dev[\sigma_{ij}]_{res} \quad (5)$$

where  $dev[\sigma_{ij}]_{res}$  is the deviatoric part of the residual stresses tensor stabilized in that grain.

The calculation of the mesoscopic stresses in Dang Van's model can be interpreted as a hardening problem, caused by elastic shakedown. When the periodic macroscopic history is represented in the deviatoric space, Dang Van assumes that the stabilized residual stress is the vector from the center of the minimum ball that circumscribes the history to the origin of the diagram. The word "ball" is used here to describe a circle, sphere or hypersphere, respectively for 2D, 3D or higher dimension histories.

The same result holds if the reduced stress  $E_{5\sigma}$  space is used, or a sub-space from it. E.g., for the 2D macroscopic deviatoric stress diagram  $S_i \times S_j$  (or a deviatoric strain

diagram  $e_i \times e_j$ , with  $1 \leq i < j \leq 5$ ) in Figure 3 on the left, the residual deviatoric stress  $\bar{s}_{res}$  (or strain  $\bar{e}_{res}$ ) is the 2D vector from the center of the circumscribed circle to the origin. It follows that the mesoscopic deviatoric history  $[S_i]_\mu \times [S_j]_\mu$  can be obtained by simply translating the origin of the macroscopic diagram to the center of the circle, see Figure 3 on the right.

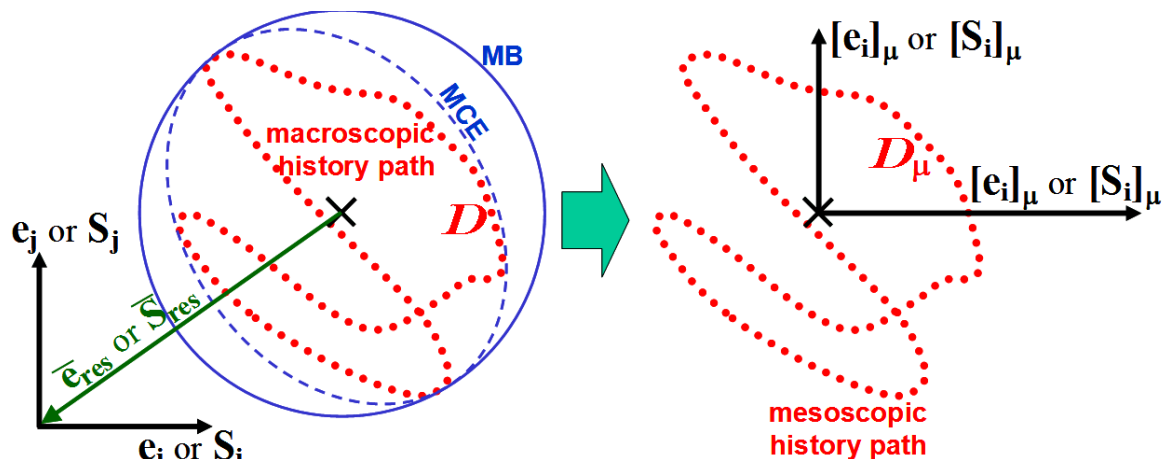


**Figure 3:** Minimum Ball (MB) and Minimum Circumscribed Ellipse (MCE) for a macroscopic path, and the resulting mesoscopic history.

The values of the mesoscopic Tresca stress  $\tau_\mu(t)$  and mesoscopic hydrostatic stress  $\sigma_{\mu h}(t)$  (which is equal to the macroscopic hydrostatic stress) are calculated for each point in the mesoscopic history path  $D_\mu$ . Dang Van then predicts infinite life if and only if all points satisfy the inequality

$$\tau_\mu(t) + \alpha_{DV} \cdot \sigma_{\mu h}(t) \leq \beta_{DV} \quad (6)$$

In summary, Dang Van is a type of Minimum Ball (MB) method where each stress state along the history path is compared to a limiting stress level to predict infinite life. However, it is not useful to calculate finite fatigue lives, since it does not deal with stress (or strain) ranges, only with individual stress states.

But the same MB circumscribed to the macroscopic history can be used to estimate an effective Mises stress range  $\Delta\sigma_{Mises}$ . The diameter  $d$  of such MB in the transformed deviatoric stress-space  $E_{5\sigma}$  (or in a 2D, 3D or 4D sub-space of such space) is the magnitude of the variation  $\Delta\bar{S}'$ , which is equal to  $\Delta\sigma_{Mises}$ . Therefore, the effective shear range  $\Delta\tau_{max}$ , Mises range  $\Delta\sigma_{Mises}$ , and octahedral shear range  $\Delta\tau_{Mises}$  can all be estimated from  $d$  using the MB method by

$$\Delta\sigma_{Mises} = 3 \cdot \Delta\tau_{Mises} / \sqrt{2} = \Delta\tau_{max} \sqrt{3} = (2\tau_a) \cdot \sqrt{3} = |\Delta\bar{S}'| = d \equiv L \cdot \lambda_{MB} \quad (7)$$

where  $L$  is the longest chord in the history (the maximum Euclidean distance in the transformed space between any two points along the history path, measured in stress units) and  $\lambda_{MB}$  is a dimensionless parameter defined as the ratio between the Mises stress range and  $L$ .

In the 2D case, if any two points from the history define the diameter of a circle that contains the entire path, then their distance  $L$  is equal to the diameter  $d$ , therefore

$\lambda_{MB} = 1.0$ . A notable 2D case is for a path forming an equilateral triangle, where  $\lambda_{MB} = 2/\sqrt{3} \cong 1.155$ . For any other 2D path, it is found that  $1.0 \leq \lambda_{MB} \leq 1.155$ .

## 5 MINIMUM ELLIPSOID METHODS

The Minimum Ball (MB) method is not efficient to represent the behavior of NP histories. For instance, it would predict the same Mises ranges for a NP 90° out-of-phase circular path and a proportional path defined by a diameter of this circle, both resulting in  $\lambda_{MB} = 1.0$ . But a higher value of  $\lambda_{MB}$  would certainly be expected for the NP history.

To solve this problem, Freitas, Li and Santos,<sup>(5)</sup> proposed the Minimum Circumscribed Ellipsoid (MCE) method. It searches for an ellipse (or ellipsoid or hyperellipsoid, for higher dimensions) that circumscribes the entire history, with its longest semi-axis  $a_1$  equal to the radius of the minimum ball, and with the smallest possible values for the remaining semi-axes  $a_i$  ( $i > 1$ ). The Mises ranges are defined by

$$\Delta\sigma_{Mises} = 2 \cdot \sqrt{\sum_{i=1}^{dim} a_i^2} \cong 2 \cdot F \quad (8)$$

where  $dim$  is the dimension of the history path,  $2 \leq dim \leq 5$ , and  $F$  is defined as the Frobenius norm of the ellipsoid, which is equal to the square root of the sum of the squares of the ellipsoid semi-axes. Here, the Frobenius norm is essentially an Euclidean distance (or Euclidean norm) between the origin and a point with coordinates  $(a_1, a_2, \dots, a_{dim})$ , since the axes of the reduced stress space are orthonormal. In the case of tensors, the Euclidean norm is commonly called the Frobenius norm, usually abbreviated as F-norm.

The ratio  $\lambda_{MCE}$  between the Mises ranges calculated by the MCE method and the longest chord  $L$  reproduces experimental data better than  $\lambda_{MB}$  generated by the MB method. In the 2D case, a NP circular path would result in  $\lambda_{MCE} = \sqrt{2}$  instead of the proportional value  $1.0$ , which is much more reasonable than the Minimum Ball prediction. It is also found that any 2D path results in  $1.0 \leq \lambda_{MCE} \leq \sqrt{2}$ , with the maximum value occurring e.g. for circular and square paths.

The downside of the MCE method is the requirement that the longest semi-axis must be equal to the radius of the Minimum Ball. For a rectangular path, this requirement results in a circle as the minimum circumscribed ellipse, with  $\lambda_{MCE} = \sqrt{2} \cong 1.414$ . But this would be true even for very elongated rectangles with very low aspect ratios between their side lengths. The MCE would thus predict  $\lambda_{MCE} = \sqrt{2}$  for an almost proportional rectangular path, instead of the expected value of  $1.0$ .

A possible alternative to the MCE method is to search for the Minimum Volume Ellipsoid (MVE), also known as the Löwner-John Ellipsoid. In the 2D case, it is basically the search for an enclosing ellipse with minimum area. Such MVE method solves the issue with rectangular paths, however it tends to find ellipses with lower aspect ratios than expected. In addition, the search for such ellipsoid or hyperellipsoid can be computationally intensive for 3D or higher dimension histories.

Another alternative to the MCE method is the search for the Minimum F-norm Ellipsoid (MFE).<sup>(6)</sup> Instead of searching for the minimum volume (or area), the MFE looks for the ellipse, ellipsoid, or hyperellipsoid with minimum value of its F-norm  $F$ , defined in Eq. (8). Zouain, Mamiya and Coules<sup>(7)</sup> present an efficient (although computationally intensive) method to numerically find such MFE.



The ratios between the Mises stress or strain ranges  $2 \cdot F$ , calculated from the MCE, MVE and MFE methods, and the longest chord  $L$  are defined, respectively, as  $\lambda_{MCE}$ ,  $\lambda_{MVE}$  and  $\lambda_{MFE}$ . All these ratios must be greater than or equal to 1.0. In the 2D case, a notable path is the one with the shape of an equilateral triangle with sides  $L$  (which are also its longest chords), where the resulting hull is a circle with diameter  $d = 2L/\sqrt{3}$  and F-norm  $F = d\sqrt{2}$ , resulting in  $\lambda_{MCE} = \lambda_{MVE} = \lambda_{MFE} = 2 \cdot F/L = 2\sqrt{2}/\sqrt{3} \cong 1.633$ . For any other 2D path, it is found that  $1.0 \leq \lambda_{MCE} \leq 1.633$  and  $1.0 \leq \lambda_{MFE} \leq 1.633$ , however  $\lambda_{MVE}$  can reach values beyond 2.0 when a very elongated enclosing ellipse is the solution with minimum area, an indication that the MVE method can be very conservative.

## 6 MAXIMUM PRISMATIC HULL METHODS

Another class of convex hull methods tries to find a rectangular prism with sides  $2a_1, \dots, 2a_{dim}$  that encloses a load history path, where  $dim$  is the dimension of the considered space. There are essentially 4 methods to fit rectangular prisms to the history path.

The first is the Maximum Prismatic Hull (MPH). This method searches for the smallest rectangular prism that encloses the history (the minimum prism), for each possible orientation of the prism. Among them, the one with highest F-norm is chosen. The F-norm and resulting Mises ranges are the same defined in Eq. (8), except that here  $a_i$  are the semi-lengths (half the length) of the sides of the rectangular prism. The MPH was originally proposed by Gonçalves, Araujo and Mamiya<sup>(6)</sup> for sinusoidal time histories, and later extended by Mamiya et al. in [8] for a general NP loading.

Another prismatic hull method is the Maximum Volume Prismatic Hull (MVPH), which searches among the minimum prisms the one with maximum volume. Although the search is for a maximum volume, the F-norm is also used to compute the Mises range. In the 2D case, the MVPH method is essentially the search, among the minimum rectangles that enclose the entire path, of the one with maximum area (it's a max-min problem).

A third method is proposed here, called the Maximum Prismatic Hull with Longest Chords (MPHLC). It is basically an improvement of Deperrois' method.<sup>(2)</sup> In the Deperrois method, the longest chord  $L_5$  between any two points of the path in the projected 5D deviatoric stress-space  $E_{5\sigma}$  is determined. Then, the path is projected onto a 4D stress-subspace  $E_{4\sigma}$  orthogonal to  $L_5$ , and the new longest chord  $L_4$  is computed in this subspace. The path is then projected onto a stress-subspace  $E_{3\sigma}$  orthogonal to both  $L_5$  and  $L_4$ , and the new longest chord  $L_3$  is computed in this subspace. Analogously, the longest chord  $L_2$  is found in the stress-subspace  $E_{2\sigma}$  orthogonal to  $L_5, L_4$  and  $L_3$ . Finally, the longest chord  $L_1$  is found in the stress-subspace  $E_{1\sigma}$  orthogonal to  $L_5, L_4, L_3$  and  $L_2$ .

The combination of the MPH and Deperrois' methods thus leads to the MPHLC method, performed in 4 steps:

- 1) define the longest side  $2a_1$  of the rectangular prism in the direction of the longest chord  $L$  of the history;
- 2) project the history into the sub-space orthogonal to the directions of all sides of the prisms that have already been defined (for a history with dimension  $dim$ , if  $m$  sides have already been chosen, then such sub-space will have  $dim-m$  dimensions);



3) define the next side  $2a_i$  of the rectangular prism in the direction of the longest chord measured in the projected sub-space, and repeat step 2 until all sides are found;

4) if multiple solutions for the rectangular prism are found, the one with maximum F-norm is chosen.

The advantage of the MPHLC method over the MPH or MVPH is that it does not require a numerical search for the prismatic hull orientation. Its orientation is deterministically defined by the longest chords. In special for 3D or higher dimension histories, the MPHLC method can lead to a huge decrease in computational effort. For instance, the orientation of a 5D hyperprism is given by 10 angles, therefore the search for the orientation associated with maximum F-norm (or maximum volume) involves a search in a 10-dimensional space, which can be very costly. In addition, the next sections will show that the MPHLC predictions give almost the same results as the MPH and MVPH methods.

A variation of the MPHLC is also proposed, called the Maximum Prismatic Hull with Container Chords (MPHCC). It is similar to the MPHLC, but all chords that contain the orthogonal projection of the entire history onto them (called here "container chords") are considered as candidate directions for the sides of the rectangular prism. Note that every longest chord LC is a "container chord" CC, but not every CC is a LC. From the probable multiple solutions for the resulting rectangular prisms, the one with maximum F-norm is chosen.

The ratios between the Mises stress or strain ranges  $2 \cdot F$ , calculated from the MPH, MVPH, MPHLC and MPHCC methods, and the longest chord  $L$  are defined, respectively, as  $\lambda_{MPH}$ ,  $\lambda_{MVPH}$ ,  $\lambda_{MPHLC}$  and  $\lambda_{MPHCC}$ . All these four ratios are, in average, very close to each other, therefore any of the four variations of the prismatic hull methods could be used interchangeably. For a history path with dimension  $dim$ , it is found that  $1 \leq \lambda_{MPHLC} \leq \lambda_{MPHCC} \leq \lambda_{MPH} \leq \sqrt{dim}$ , therefore the MPHCC results in Mises ratios slightly closer to the MPH predictions than the MPHLC. In addition, it is also found that  $1 \leq \lambda_{MVPH} \leq \lambda_{MPH} \leq \sqrt{dim}$ .

In the next section, all convex hull methods presented in this paper are evaluated and compared.

## 7 COMPARISON AMONG THE CONVEX HULL METHODS

Figure 4 shows the convex hulls obtained from all presented methods for a rectangular history path in a reduced 2D sub-space, and their ratios  $\lambda$  between the Mises ranges and longest chord  $L$ . Note that, in this example,  $L$  is the diagonal of the rectangular path.

Experimental results suggest that the expected ratio  $\lambda$  in this example is about 1.3. However, the MB method predicts  $\lambda_{MB} = 1.0$ , which is very non-conservative. The MB assumes that such rectangular path would have the same Mises range  $L$  as a straight path along one of its diagonals, which is not reasonable. The MCE method, on the other hand, overestimates  $\lambda$ , obtaining  $\lambda_{MCE} = \sqrt{2} \cong 1.414$ . The MCE method finds the same circle from the MB to enclose such history, even though the aspect ratio of this rectangular path is very different from 1.0, suggesting instead the use of an elongated elliptic hull.

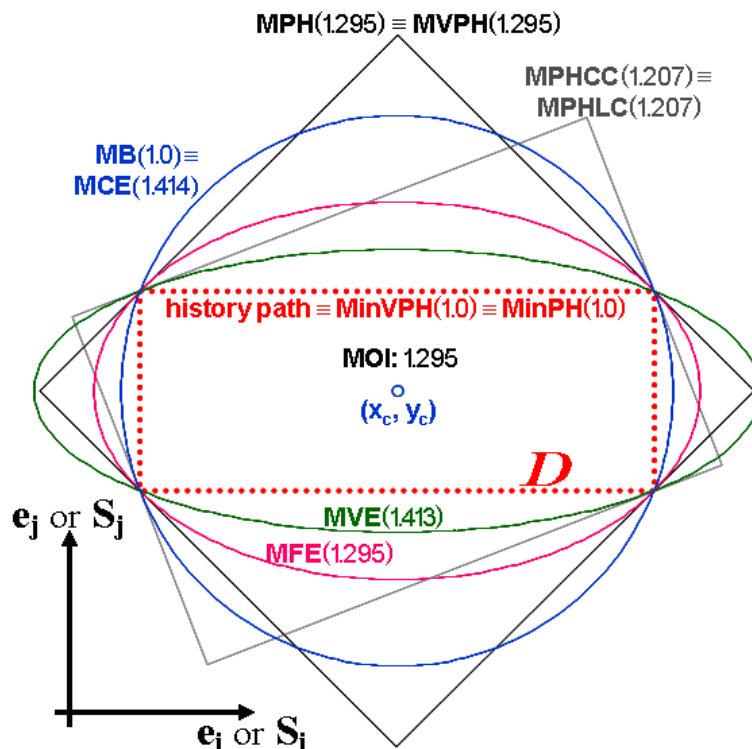


**Figure 4:** Values of the  $\lambda$  Mises stress (or strain) range ratio for the MB, MCE, MVE, MFE, MPH, MPHLC, MPHCC, MVPH, MinPH, MinVPH and MOI methods for a rectangular 2D history path.

The MVE method also tends to overestimate  $\lambda$ , obtaining in this example  $\lambda_{MVE} = 1.413$ . In the search for the minimum area (or volume, for higher dimension diagrams), the MVE method ends up finding overly elongated ellipses ( $b \ll a$ ), which have a small area  $\pi \cdot a \cdot b$  due to the very low value of  $b$  but an unrealistically high F-norm  $(a^2 + b^2)^{1/2}$  due to the high value obtained for  $a$ . Thus,  $\lambda_{MVE}$  overestimates the ratio  $\lambda$ , since it is calculated from this unrealistic F-norm, and not from the area (or volume).

Among the ellipsoid hull methods, the MFE gives the best predictions, resulting in  $\lambda_{MFE} = 1.295$ , with an enclosing ellipse with a much more reasonable aspect ratio than the ones from the MCE and MVE methods, see Figure 4.

Both MPH and MVPH methods obtain in this example  $\lambda_{MPH} = \lambda_{MVPH} = 1.295$ , which exactly agrees with the MFE prediction. Note however that the MPH and MFE methods are not equivalent, since they result in slightly different  $\lambda$  values between them for other history paths, as shown in Castro et al.<sup>(9)</sup>

The MPHLC and MPHCC result in  $\lambda_{MPHLC} = \lambda_{MPHCC} = 1.207$ , a value about 7% lower than the MPH prediction. The fact that  $\lambda_{MPHLC} \leq \lambda_{MPH}$  and  $\lambda_{MPHCC} \leq \lambda_{MPH}$  is not a surprise, since the MPH searches for the maximum F-norm checking rectangles (in the 2D case) in all directions, while the MPHLC and MPHCC only search for rectangles in the directions of the longest and/or container chords. If these directions of longest or container chords coincide with the ones associated with a maximum F-norm rectangle (which is quite often true), then the MPHLC or MPHCC predictions will coincide with  $\lambda_{MPH}$ , otherwise they will result in  $\lambda$  ratios slightly lower than the upper bound  $\lambda_{MPH}$ .

Figure 4 also shows the prismatic hulls MinPH and MinVPH with minimum (instead of maximum) F-norm and volume (or area, in 2D), respectively. In this example, these rectangular hulls would coincide with the original rectangular path, wrongfully predict-



ing  $\lambda = 1$ . This counter-example shows why no prismatic hull method with minimum F-norm or volume has been proposed.

In summary, the MB method tends to underestimate the Mises stress or strain range ratio  $\lambda$ , while the MCE and MVE overestimate it. The MPHLC and MPHCC slightly underestimate  $\lambda$ , while the MFE, MPH and MVPH give very similar (although, in general, different) predictions.

But the above considerations are based on a single example. To really compare all convex hull methods, it is necessary to study all possible history path topologies in 2D, 3D, 4D and 5D deviatoric stress or strain spaces. Monte Carlo simulations are performed for  $3 \cdot 10^6$  random 2D history paths, in addition to a few selected paths to try to cover all possible path topologies. All convex hull methods are applied to each of these simulated paths, to evaluate and compare the  $\lambda$  predictions. The following discussions focus on 2D paths, however similar conclusions are found for 3D, 4D and 5D histories.

The simulations show that the MPHCC tends to underestimate  $\lambda$  when compared to the MPH, as expected. For 2D paths, in average,  $\lambda_{MPHCC}$  is about 98% of  $\lambda_{MPH}$ , with a standard deviation of only 2%. Also,  $\lambda_{MPHCC}$  never underestimates  $\lambda_{MPH}$  by more than 10%. In addition, the MPHLC and MPHCC usually give almost identical results, with  $\lambda_{MPHLC}$  being in average about 99.85% of  $\lambda_{MPHCC}$ , with a standard deviation of only 0.9% for these  $3 \cdot 10^6$  simulations. In addition, the MPH and MVPH have a very good agreement, except for low values of  $\lambda$ . It is found that  $\lambda_{MVPH} \leq \lambda_{MPH}$  and, in average,  $\lambda_{MVPH}$  is about 98.6% of  $\lambda_{MPH}$ , with a standard deviation of only 1.8%.

The MPH and MFE methods are coherent, however they can lead to very different  $\lambda$  predictions. It is found that  $\lambda_{MFE} \geq \lambda_{MPH}$  and, in average,  $\lambda_{MPH}$  is about 92.9% of  $\lambda_{MFE}$ , with a standard deviation of 4.3%.

The MVE method can severely (and wrongfully) overestimate  $\lambda$ , in special for low values of  $\lambda_{MPH}$ , associated with almost proportional paths. As discussed before, almost proportional paths can lead to overly elongated ellipses in the MVE method, which can have a small area but an unrealistically large F-norm, leading to  $\lambda_{MVE}$  values larger than 2.0 in some extreme cases.

Also, it is found that  $\lambda_{MCE}$  overestimates  $\lambda$ , in special for low values of  $\lambda_{MFE}$ , associated with almost proportional paths. For instance, for an almost proportional history defined by a rectangular path with very low aspect ratio, the expected  $\lambda$  would be close to 1.0 (which is the expected value of  $\lambda$  for proportional histories), however the MCE method would circumscribe a circle (instead of an elongated ellipse) to such elongated rectangular path, wrongfully predicting  $\lambda_{MCE} = \sqrt{2}$ , revealing the inadequacy of the MCE method.

Finally, the MB method can severely (and wrongfully) underestimate  $\lambda$ , except for almost proportional load histories (where  $\lambda_{MB} \cong \lambda_{MFE} \cong 1.0$ ).

## 8 CONCLUSIONS

In this work, all convex hull methods from the literature were reviewed and compared, and new methods were proposed. The conclusions from the comparisons are:

1. the prismatic hull methods MPHLC and MPHCC are very similar to the MPH and MVPH methods, but with a much simpler search algorithm for 3D to 5D histories;
2. the only recommended ellipsoid hull is the Minimum F-norm Ellipsoid (MFE), which results in similar (but not equal)  $\lambda$  predictions when compared to the prismatic hull methods; and



3. the Minimum Circumscribed Ellipsoid (MCE), Minimum Volume Ellipsoid (MVE), and Minimum Ball (MB) methods may result in very poor predictions of the stress or strain amplitudes.

In summary, the Minimum F-norm Ellipsoid and all four Maximum Prismatic Hull (MPH) models are efficient to predict equivalent amplitudes in NP histories, even though they do not perform well in cross or star-shaped paths, as it will be shown from experimental results in Part II of this paper.

### Acknowledgements

CNPq has provided research scholarships for the authors.

### REFERENCES

- 1 SOCIE, D.F.; MARQUIS, G.B. *Multiaxial Fatigue*, SAE 1999
- 2 DEPERROIS, A., *Sur le calcul des limites d'endurance des aciers*. Thèse de Doctorat. Ecole Polytechnique, Paris, 1991
- 3 KIDA, S.; ITOH, T.; SAKANE, M.; OHNAMI, M.; SOCIE, D.F. Dislocation structure and non-proportional hardening of type 304 stainless steel, *Fatigue and Fracture of Engineering Materials and Structures*, v.20, n.10, p.1375-86, 1997
- 4 DANG VAN, K.; PAPADOPOULOS, I.V. *High-Cycle Metal Fatigue*. Springer 1999
- 5 FREITAS, M.; LI, B.; SANTOS, J.L.T. *Multiaxial Fatigue and Deformation: Testing and Prediction*, ASTM STP 1387, 2000
- 6 GONÇALVES, C.A.; ARAÚJO, J.A.; MAMIYA, E.N. Multiaxial fatigue: a stress based criterion for hard metals, *Int.J.Fatigue* v.27, p.177-87, 2005
- 7 ZOUAIN, N.; MAMIYA, E.N.; COMES, F. Using enclosing ellipsoids in multiaxial fatigue strength criteria, *European J. of Mech. - A, Solids*, v.25, p.51-71, 2006
- 8 MAMIYA, E.N.; ARAÚJO, J.A.; CASTRO, F.C. Prismatic hull: A new measure of shear stress amplitude in multiaxial high cycle fatigue, *Int.J.Fatigue*, v.31, p.1144-53, 2009
- 9 CASTRO, F.C.; ARAÚJO, J.A.; MAMIYA, E.N.; ZOUAIN, N. Remarks on multiaxial fatigue limit criteria based on prismatic hulls and ellipsoids, *Int.J.Fatigue*, v.31, p.1875-81, 2009